

Accepted Manuscript

Synthesis and structure-activity relationships of novel arylpiperazines as potent antagonists of α 1-adrenoceptor

Renata Oliveira Silva, Andressa Souza de Oliveira, Laís Flávia Nunes Lemes, Luciana de Camargo Nascente, Patrícia Coelho do Nascimento Nogueira, Edilberto R. Silveira, Guilherme D. Brand, Giulio Vistoli, Antonio Cilia, Elena Poggesi, Michela Buccioni, Gabriella Marucci, Maria Laura Bolognesi, Luiz Antonio Soares Romeiro



PII: S0223-5234(16)30542-6

DOI: [10.1016/j.ejmech.2016.06.052](https://doi.org/10.1016/j.ejmech.2016.06.052)

Reference: EJMECH 8713

To appear in: *European Journal of Medicinal Chemistry*

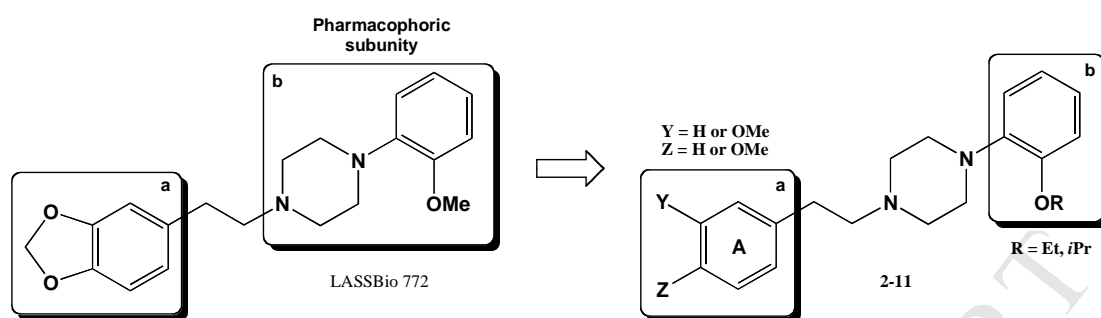
Received Date: 25 February 2016

Revised Date: 10 June 2016

Accepted Date: 28 June 2016

Please cite this article as: R.O. Silva, A.S. de Oliveira, L.F. Nunes Lemes, L. de Camargo Nascente, P. Coelho do Nascimento Nogueira, E.R. Silveira, G.D. Brand, G. Vistoli, A. Cilia, E. Poggesi, M. Buccioni, G. Marucci, M.L. Bolognesi, L.A. Soares Romeiro, Synthesis and structure-activity relationships of novel arylpiperazines as potent antagonists of α 1-adrenoceptor, *European Journal of Medicinal Chemistry* (2016), doi: 10.1016/j.ejmech.2016.06.052.

This is a PDF file of an unedited manuscript that has been accepted for publication. As a service to our customers we are providing this early version of the manuscript. The manuscript will undergo copyediting, typesetting, and review of the resulting proof before it is published in its final form. Please note that during the production process errors may be discovered which could affect the content, and all legal disclaimers that apply to the journal pertain.



Synthesis and Structure–Activity Relationships of Novel Arylpiperazines as Potent Antagonists of α_1 -Adrenoceptor

Renata Oliveira Silva,^{a, b} Andressa Souza de Oliveira,^{a, b} Laís Flávia Nunes Lemes,^b Luciana de Camargo Nascente,^b Patrícia Coelho do Nascimento Nogueira,^c Edilberto R. Silveira,^c Guilherme D. Brand,^d Giulio Vistoli,^e Antonio Cilia,^f Elena Poggesi,^f Michela Buccioni,^g Gabriella Marucci,^g Maria Laura Bolognesi,^{h,*} Luiz Antonio Soares Romeiro^{a, b *}

^a *Department of Pharmacy, Health Sciences Faculty, University of Brasília, Campus Universitário Darcy Ribeiro, 70910-900, Brasília, DF, Brazil*

^b *LADETER, Catholic University of Brasília, QS 07, Lote 01, EPCT, Águas Claras, 71966-700, Brasília, DF, Brazil*

^c *Department of Organic and Inorganic Chemistry, Federal University of Ceará, 60021-970, Fortaleza, CE, Brazil*

^d *Chemistry Institute, University of Brasília, Campus Universitário Darcy Ribeiro, 70910-900, Brasília, DF, Brazil*

^e *Department of Pharmaceutical Science, University of Milan, Via Mangiagalli 25, 20133, Milan, Italy.*

^f *Drug Discovery Department, Recordati S.p.A. Via Civitali 1, 20148 Milan, Italy*

^g *School of Pharmacy, Medicinal Chemistry Unit, University of Camerino, via S. Agostino, 1, I-62032, Camerino, Italy*

^h *Department of Pharmacy and Biotechnology, University of Bologna, Via Belmeloro 6, 40126 Bologna, Italy*

Key words: adrenergic receptors subtypes, BPH, α_1 -adrenergic antagonists, arylpiperazines

* Corresponding author: Phone +61 3107 1620; e-mail, luizromeiro@unb.br

* Corresponding author: Phone +39 051 2099717; e-mail, marialaura.bolognesi@unibo.it

Abstract

Arylpiperazines **2-11** were synthesized, and their biological profiles at α 1-adrenergic receptors (α 1-ARs) assessed by binding assays in CHO cells expressing human cloned subtypes and by functional experiments in isolated rat vas deferens (α 1A), spleen (α 1B), and aorta (α 1D). Modifications at the 1,3-benzodioxole and phenyl pharmacophoric units resulted in the identification of a number of potent compounds (moderately selective with respect to the α 1b-AR), in binding experiments. Notably, compound **7** (LDT451) showed a subnanomolar pK_i of 9.41 towards α 1a-AR. An encouragingly lower α 1B-potency was a general trend for all the series of compounds, which showed α 1A/D over α 1B selectivity in functional assays. If adequately optimized, such peculiar selectivity could have relevance for a potential LUTS/BPH therapeutic application.

1. Introduction

α 1-Adrenergic receptors (α 1-ARs^a), activated by norepinephrine (NE), play important roles in cardiovascular and urogenital physiology.¹ They also represent one of the most investigated families of class A G protein coupled receptors (GPCRs).

The family encompasses at least three distinct subtypes (α 1A, α 1B, and α 1D), which differs for their biological structure, tissue distributions, pharmacological properties, and signal transduction. In the past, studies aimed to assess the specific functional responses mediated by each α 1-AR subtype have been hindered by the lack of truly subtype-selective drugs.² More recently, studies on genetically modified mice lacking or overexpressing one or more α 1-AR subtypes have shed some light on the functional roles played by distinct receptors. However, our understanding on the functional implications of α 1-AR heterogeneity in physiological systems is still quite limited.³

In addition to their importance from a chemical biology perspective, α 1-ARs are validated drug targets for current drug discovery.² Indeed, several studies confirmed that α 1-ARs are critically involved in benign prostatic hyperplasia (BPH), hypertension, prostate cancer, and other diseases representing currently unmet medical needs.⁴

In particular, the alpha-blocker therapy for BPH dawned in the mid 1970s with the use of nonselective agents, such as phenoxybenzamine. The therapeutic options have then expanded significantly, giving rise to the receptor-specific alpha-blockers that encompass nowadays the first line of therapy. They treat the dynamic component of BPH by blocking α 1-receptor-mediated sympathetic stimulation to relax the smooth muscle in the prostate. Tamsulosin (Fig. 1) is a subtype-selective α 1A- and α 1D-adrenoceptor antagonist that demonstrated advantages over older and less selective agents,⁵ in the management of patients with lower urinary tract symptoms (LUTS)

^a Abbreviations: α 1-ARs, α 1-adrenergic receptors; BPH, benign prostatic hyperplasia; CHO, Chinese hamster ovary; GPCRs, G protein coupled receptors; HBA, H-bond acceptor; IR, infrared; LUTS, lower urinary tract symptoms; MW, microwave; NE, norepinephrine; SAR, structure-activity relationships.

associated with BPH.⁶ Silodosin (Fig. 1) is a recently approved α 1A antagonist that exhibits an even improved selectivity among the α 1-adrenoceptor subtypes. Its exceptionally high *in vitro* selectivity for α 1A- versus α 1B-adrenoceptors, likely accounts for the very favorable tolerability profile.⁷ Indeed, both preclinical and clinical studies support the assertion that silodosin markedly reduces dynamic neutrally mediated smooth muscle relaxation in the lower urinary tract while minimizing undesirable effects on blood pressure regulation.

All in all, the search for new α 1-antagonists as both molecular probes⁸ and drug candidates is still an active area of medicinal chemistry research.

Arylpiperazines represent one of the most studied classes of α 1-AR antagonists. This class includes a considerable variety of compounds that are characterized by a common arylpiperazine scaffold, linked through a proper polymethylene spacer to various heteraromatic moieties.² In previous works, some of us reported that a series of 1-phenylpiperazines bind with high affinity to α 1-ARs in both binding and functional assay.⁹ In particular, the congener carrying a 2-methoxyphenyl moiety on the piperazine ring and a 1,3-benzodioxole as a second pharmacophoric unit, named LASSBio-772 (**1** in Chart 1), was the most active of the series. It showed a remarkable pK_i of 9.85 for the rat α 1A-AR, a value similar to that displayed by tamsulosin ($pK_i = 9.89$).⁹ The measured pK_i of 8.25 for the α 1B-subtype gave rise to 40-fold higher affinity for α 1A-AR. **1** also presented high affinity ($pK_B = 10.60$) for the α 1D-AR subtype in the functional rat aorta assay, showing to be equipotent to tamsulosin ($pK_B = 10.78$).⁹

A similar high activity towards α 1A-AR was found for another 1-(2-methoxyphenyl)piperazine derivative developed by some of us, *i.e.* LDT66.¹⁰ In particular, this derivative simultaneously blocked both the α 1A- and α 1D-adrenoceptors and the 5-HT1A receptors *in vitro* and *in vivo*, and has therefore been proposed as a multi-target ligand for the treatment of BPH and LUTS.¹⁰

These recent findings prompted us to investigate whether derivatives of **1** have the capacity for more selective discrimination among the different α 1-AR subtypes. Thus, we thought of interest to verify if modification in the 1-(2-methoxyphenyl)piperazine group and/or in the 1,3-benzodioxole

moiety could lead to an improvement of the affinity profile for α 1-adrenoceptors, and, hopefully, of the therapeutic application. Particularly (Chart 1), the 2-methoxy substituent of **1** was replaced with an ethoxy or isopropoxy one to increase at different extent the steric hindrance and the hydrophobic properties of the parent compound. To note, the isopropoxy substituent has revealed a key feature of some known potent and selective α 1-adrenoceptor antagonists.^{11, 12} In addition, we evaluated the effects of opening the 1,3-benzodioxole ring, by synthesizing the corresponding acyclic analogues, with different H-bond acceptor (HBA) contribution patterns. Here we report the synthesis of compounds **2-11** together with their affinity profiles assessed by binding assays in cells expressing human cloned α 1-AR subtypes, and by functional experiments in isolated rat vas deferens (α 1A), spleen (α 1B), and aorta (α 1D). Their putative binding mode at the three subtypes was also explored, by molecular modeling simulations.

2. Chemistry

The novel series of derivatives (**2-11**) were prepared by straightforward S_N2 methodologies, exploiting phenethyl bromides (**12-16**) and 1-(2-alkoxyphenyl)piperazines (**17-19**) as starting reagents (Scheme 1).

The required 5-(2-bromoethyl)-1,3-benzodioxole (**12**) was synthesized through the reduction of (1,3-benzodioxol-5-yl)acetic acid (**20**) with lithium aluminum hydride in tetrahydrofuran, to afford the alcohol **21**⁹ in 98% yield. Next, treatment of **21** with CBr_4 and triphenylphosphine in acetonitrile furnished the target bromide **12** in 76% yield (Scheme 2). Conversely, the unsubstituted-phenethyl (**13**), 3-methoxyphenethyl (**14**), 4-methoxyphenethyl (**15**) and 3,4-dimethoxyphenethyl (**16**) bromides were commercially available.

As for the 1-(2-alkoxyphenyl)piperazine starting fragments, 1-(2-methoxyphenyl)piperazine **17** and 1-(2-ethoxyphenyl)piperazine **18** were purchased by commercial vendors, whereas 1-(2-isopropoxyphenyl)piperazine **19** was synthesized as previously reported.¹³

Bromides **12-16** were then converted into final compounds **2-11** following nucleophilic displacement with the proper 1-(2-alkoxyphenyl)piperazine (**17-19**) in acetonitrile, under irradiation in a microwave (MW) oven (operating at 2.45 GHz, 450 W) for 4 minutes (Scheme 1).

All compounds described herein gave analytical and spectral data in agreement with the proposed structures.

3. Biology

3.1 Binding Experiments. First, the affinity profile of compounds **2-11** was evaluated by radioreceptor binding assays using **1** and tamsulosin as reference compounds. [³H]Prazosin was used to label α_1 -adrenoceptor binding sites on membranes of Chinese hamster ovary (CHO) cells expressing human α_{1A} , α_{1B} , and α_{1D} -adrenoceptor subtypes. Binding affinities were expressed as pK_i values derived using the Cheng–Prusoff equation, as previously reported.¹⁴

3.2 Functional Studies. Receptor subtype selectivity of compounds **2-9** and **11** was also determined at α_1 -ARs on different isolated rat tissues, using **1** and tamsulosin as reference standards. α_1 -AR subtypes blocking activity was assessed by antagonism of (-)-NE-induced contraction of rat prostatic vas deferens (α_{1A}), rat spleen (α_{1B}), or thoracic aorta (α_{1D}). The potency was expressed by the pK_B value (with the exception of compound **7**), according to van Rossum, and was calculated at the lowest antagonist concentration giving a significant rightward shift of the agonist concentration-response curve [$\log(\text{concentration ratio} - 1) \geq 0.5$]. For compound **7** pA_2 values at all adrenoceptor subtypes were calculated from Schild plot.

4. Results and discussion

Our main goal in this study was to explore structure-activity relationships (SAR) around LASSBio-772, a highly potent α_1 -AR antagonist. We thus sought to assess how modifying the pharmacophoric features of **1**, *i.e.* the 1,3-benzodioxole and the phenylpiperazine moieties, could affect the antiadrenergic profile. To this end, the inhibitory affinities of **2-11** were first evaluated on

human recombinant α_1 -AR. For a better comparison of the results, **1** and tamsulosin were used as reference compounds (Table 1). To note, the inhibitory profile of **1** on human cloned receptors has never been reported before. However, with human receptor clones available, collecting data from single human proteins from the inception of a project would be undoubtedly more relevant from a drug discovery point of view.

As matter of fact, we should remark that **1** showed a significant affinity profile even at human subtypes, with K_i values in the single-digit nanomolar range. As regard as selectivity, **1** displayed a slightly higher affinity for the α_{1d} -adrenoceptor with respect to α_{1a} and α_{1b} subtypes (2.5- and 4-fold, respectively). Next, the data obtained for compound **2** clearly highlight the role of the 1,3-benzodioxole moiety of **1**. Indeed, the presence of an unsubstituted phenyl ring in **2** and **8** resulted in a general drop of affinity with respect to the benzodioxole derivative (compare **1** vs **2** and **7** vs **8**). This drop was more marked for the α_{1b} -subtype, giving raise to a slight selectivity ratio.

An encouragingly lower α_{1b} -affinity was a common trend for all the compounds, which, like **1**, showed a similar (albeit modest) $\alpha_{1a/d}$ over α_{1b} selectivity. This is a positive feature for the potential application of these molecules in the treatment of BPH, as it leads to a reduced incidence of cardiovascular side-effects (see below).

Conversely, the opening of the dioxole ring, affording 3-methoxy- (**4**, **9**), 4-methoxy- (**5**, **10**) or 3,4-dimethoxy-phenyl derivatives (**6**, **11**), only slightly affected inhibition. Intriguingly, the 3,4-disubstituted phenyl turned out an optimal substituent for α_{1d} recognition, with compound **6** resulting the most active of the series against this subtype. In details, it showed an excellent subnanomolar affinity, with a pK_i of 9.22, higher than that of **1** (pK_i of 8.90).

To examine the influence of the 2-phenyl substituent on the affinity and selectivity of Lassbio-772 at α_1 -AR, **3** and **7** were synthesized. As expected, the sterically bulkier 2-isopropoxy moiety of **7** (adopted from RWJ 37914)¹¹ was superior to the less bulky 2-ethoxy (**3**) or 2-methoxy (**1**) for both α_{1a} -AR binding affinity ($pK_i = 9.41$ nM for **7** vs 8.95 for **3** or 8.46 for **1**) and selectivity (α_{1a}/α_{1b} 32-fold versus 5-fold or 1.5-fold; $\alpha_{1a}/\alpha_{1d} = 0.2$ -fold versus 0.5-fold or 2.5-fold, respectively).

Indeed, **7** was the most active α 1a-ligand, confirming that this substituent can optimally fit in a hydrophobic subpocket, which is peculiar to the α 1a-subtype. Conversely, the slightly reduced potency of **7** at α 1b-subtype could be related to the increased steric hindrance of the isopropoxy in comparison with the methoxy moiety of **1**, at this receptor site.

In summary, in binding assays the optimization at the X, Y, and R positions of **1** (Chart 1) resulted in the identification of a number of equally or slightly more potent and more selective compounds than **1** with respect to the α 1b-AR.

Motivated by these interesting results, the synthesized compounds were also tested in functional assays for their activity at α 1-AR subtypes in isolated rat prostatic vas deferens (α 1A-AR), spleen (α 1B) and thoracic aorta (α 1AD-AR). Their pK_B values, along with those of **1** and tamsulosin, are listed in Table 2. We were pleased to observe that all compounds, in analogy with what reported for **1**,⁹ behaved as competitive antagonists. In fact, the concentration–response curves of reference agonists after and before incubation with the tested compounds were parallel with no reduction of the maximal effect, and the shift produced was proportional to the concentrations used.

However, we should highlight that in our hands **1** resulted significantly less potent in blocking NE-induced contractions of rat thoracic aorta strips than what was reported before.⁹ One possible explanation for the difference observed in the two studies could be attributed to the different tissue preparation and the experimental conditions chosen in the assays. In particular, in the rat aorta strips preparation all endothelium is preliminary removed, by rubbing the luminal surface, in order to avoid the slight endothelium-dependent vasorelaxation through the stimulation of α 1D-AR located on endothelial cells.¹⁵ Moreover, the presence of cocaine, a known inhibitor of NE reuptake, provides a higher endogenous agonist concentration at the receptor, influencing the dose-response curve.

Encouragingly, **1** exhibited a functional profile very similar to that disclosed in binding experiments. However, the results obtained in functional assays did not match the affinity profile observed in binding studies for all the synthesized derivatives. It can be easily seen that pK_B values

derived from functional experiments of compounds **2-4** and **8, 9** and **11** are quantitatively in disagreement with binding affinities. In particular, a general lower affinity with respect to that found in binding occurred at the α 1D-AR subtype. Conversely, functional profiles of **6** and **7** differ from binding data both qualitatively and quantitatively. Specifically, **6**, in functional assays, showed a decrease in affinity at the α 1D-AR together with a consistent concomitant increase at the α 1A-AR, resulting in an inversion of the selectivity profile. On the other hand, **7** showed a negative shift in potency at α 1A of 14-fold (pK_i of 9.41 vs pK_B of 8.27).

As previously proposed by Melchiorre et al.,¹⁶ the apparent discrepancy between binding and functional data can be explained by considering the following: (i) these compounds act as inverse agonists, and hence their affinity is system-dependent (just as does observed potency for positive agonists)¹⁷; (ii) receptor form homo- and/or heterodimers, and hence native receptors in functional tissues can be organized differently than cloned receptors (iii) species differences (human vs rat) ; (iv) a different bioavailability of the compounds at the receptor level.

To rule out the first possibility, for compound **7**, pA_2 values at all adrenoceptor subtypes were calculated from Schild plot.^{14, 18} Results showed that **7** behaves as competitive antagonist at α 1A adrenoceptor with a pA_2 of 8.38 ± 0.11 , but it is not a competitive antagonist at the other subtypes. These findings allow excluding that it acts as an inverse agonist since inverse agonist binds to the same agonist receptor binding-site and the increase of agonist concentration restores the receptor activity. On the other hand, a non-competitive antagonist may not interact with the same neurotransmitter binding-site and it is impossible to have the full response of the receptor even in the presence of high concentration of agonist. In conclusion, the different behavior of compound **7** in binding and functional assays could be due to its interaction with a binding site different from that of NE on α 1B, and α 1D adrenoceptor subtypes.

To get further clues on these issues, we undertook docking simulations for molecules **2-11** by using AR homology models. As further discussed in the supporting information (see also), we noticed that the ligands can assume two predominant “symmetrical” binding poses, depending on the

contact of the protonated nitrogen (ammonium head): the first is characterized by canonical interaction with Asp106 and Tyr316, while the second involves a similar dyad of interacting residues (Glu180 and Gln177); in both cases, the ligand can establish a key ion-pair reinforced by H-bonds. Also the two lateral pockets accommodating the phenyl rings showed a certain degree of symmetric similarity. As exemplified for **9** in Figure 2A, a first binding mode is stabilized by the key ion-pair between the ammonium head and Asp106 reinforced, as mentioned above, by a H-bond with Tyr316. The phenethyl group is inserted into a lateral subpocket where it can stabilize π - π stacking interactions with Phe288 and Phe289 reinforced by hydrophobic contacts with Val107 and Ile178, while the methoxy substituent can elicit H-bonds with Ser188 and Ser192 plus apolar interactions with the above cited alkyl side chains. Finally, the phenyl ring connected to the piperazine is harbored within the second lateral subpocket where it is engaged in π - π stacking interactions with Phe86 and Trp102, while the isopropoxy group elicits a H-bond with Gln177 plus hydrophobic contacts with Phe308 and the carbon skeleton of Lys309. The second “symmetric” binding mode observed for **9** is depicted in Figure 2B and is stabilized by the following set of contacts: (1) the ion pair between the ammonium head and Glu180 reinforced by a H-bond with Gln177; (2) the phenethyl group approaches Phe86 and Trp102 and the methoxy substituent elicits a H-bond with Ser83 and (3) the phenyl ring connected to the piperazine contacts Phe288 and Phe289 and the isopropoxy group stabilizes H-bonds with Ser188 and Ser192. A systematic analysis of the best computed poses for all simulated ligands revealed that the two different arrangements (and so the different contacts) of the ammonium head is the distinctive feature which characterizes the monitored binding modes, while the specific pose of the two aromatic systems can vary, depending on their steric hindrance and their capacity to stabilize H-bonds.

The possibility of two distinct arrangements with which the ammonium head interacts with the α 1a binding site is particularly relevant when considering that the role of Asp106, despite being the most conserved negatively charged residue among the aminergic GPCRs, is largely debated. The available mutational analyses reported contradictory results and, in particular, a recent study

unambiguously demonstrated that mutations involving Asp106 have no significant effects on antagonists's affinity.¹⁹ The here reported existence of an alternative negatively charged residue (Glu180) which can replace Asp106 might explain the still questioned role of Asp106, thus suggesting that the two described binding modes can equally contribute in determining ligand affinity. Clearly, the specific role of the two binding modes in influencing the ligand potency remains to be clarified. To this end, a correlative analysis was performed, which suggest that both binding modes contribute to ligand affinity (see the SI for experimental details) even though that involving Asp106 seems to play a predominant role.

The correlations involving the potency values show different trends, since the relationship involving the pose with Asp106 is clearly better than the corresponding correlation with affinity values, while those involving the second binding mode or the average values perform largely worst. Taken together, these results suggest that the potency is almost exclusively induced by the pose involving Asp106 and, more importantly, the remarkable correlation involving the difference values underlines that the other possible poses represent a side effect, the stability of which reduces the measured potency. Overall, these results might explain the above mentioned contradictory results coming from mutagenesis and suggest that, while the ligand affinity benefits of all binding modes a ligand can assume, the ligand potency is strongly dependent by selected effective poses (such as that involving Asp106). This also suggests that the ligand potency can be optimized by rendering less favored the binding modes not involving Asp106. For example, the notable potency of **9** and **11** seems to indicate that an increased steric hindrance in both phenyl systems tends to disfavor the ineffective pose involving Glu180. Such a symmetric architecture of the binding site, despite less noticeable, is still present in $\alpha 1b$ and $\alpha 1d$ subtypes as evidenced by the corresponding docking results which can be found in SI.

We also performed the *in silico* physico-chemical profiling (solubility, ionization, lipophilicity, permeability) of the newly synthesized compounds to predict their pharmacokinetic properties (see Table 2 in SI).

Finally, to get preliminary clues on the cellular profile of the current series, the effect of **7** on prostate cell growth was evaluated *in vitro*. Indeed, previous studies reported that treatment of PC-3 prostate cancer cells with α_1 -antagonists doxazosin and terazosin results in a significant loss of cell viability, whereas tamsulosin had no effect.²⁰ In agreement with these findings, we did not observe any antiproliferative effect for compound **7** in a range of concentration from 0.01 to 10 μ M. These data seem to confirm that the described capability of inhibiting prostate cell growth is independent from the α_1 -antagonist properties, and it likely resides in the quinazoline chemotype common to doxazosin and terazosin.

4. Conclusions

In the current work, we have described a series of novel 1-phenylpiperazines related to hit compound **1**, which show high affinity and potency towards α_1 -adrenoceptors. The added SAR trends help to define the structural features involved in optimal recognition at the different receptor subtypes for this class of molecules. The investigation of the binding mode for **2-11** provides an explanation for these results, and the molecular insights of receptor-ligand interactions gained from the performed docking study can be exploited for the development of novel derivatives. Of note, the $\alpha_{1A/D}$ over α_{1B} selectivity disclosed for most of the compounds, albeit modest, could have relevance for a potential LUTS/BPH therapeutic application. This is because of the proposed more beneficial treatment effects deriving from the preferential antagonism of the α_{1A} -adrenoceptor, which relieves the voiding symptoms due to the bladder outlet obstruction mediated by prostate smooth muscle contraction, and from a concomitant effective antagonism towards the α_{1D} subtype, which alleviates the symptoms of bladder filling. At the same time, the lower activity at the α_{1B} -adrenoceptor of the arterial vessels should minimize the blood pressure-related adverse effects, such as orthostatic hypotension.⁵

Indeed, compound **3** (LDT8) has been selected for a more detailed pharmacological characterization aimed to disclose its therapeutic potential in the treatment of BPH.²¹ Notably, it showed a low

affinity (micromolar range) for receptors unrelated to BPH such as α 2A-adrenoceptors, muscarinic and 5-HT_{2A} receptors, which is a desirable profile in terms of putative side effects.²¹

Based on the considerations above and also considering the simpler and achiral structures of the current phenylpiperazines with respect to those marketed for BPH (*i.e.* tamsulosin and silodosin), **2-11** provide a good starting point in the design of novel analogues for BPH.

5. Experimental

5.1. Chemistry. General information

Melting points were determined on a Quimis MQAPF 302 apparatus and are uncorrected. Infrared (IR) spectra were obtained on a Perkin Elmer – Spectrum BX infrared spectrophotometer. ¹H and ¹³C NMR spectra were recorded on Bruker Avance DRX500 or DRX300 instruments. Chemical shifts (δ) are expressed in parts per million relative to internal tetramethylsilane; coupling constants (J) are in Hertz. Microanalyses were obtained with Thermofinnigan EA1112 analyzer, using a Metler MX5 electronic balance. Reactions were routinely monitored by thin-layer chromatography (TLC) in silica gel (F254 Silicycle plates) and the products visualized with iodine or ultraviolet lamp (254 and 365 nm). For normal pressure and flash column chromatography purifications, Silicycle silica gel type 60 (size 70-230 and 230-400 mesh, respectively) was used. Unless stated otherwise, starting materials used were high-grade commercial products. The purity of the final compounds was assessed by a Biotage Isolera One System and was found > 95%. HRMS spectra were acquired on a TripleTof 5600+ (Sciex, Ontario, Canada) by flow injection analysis using a liquid chromatographer (Eksigent UltraLC 100, Sciex) set to a flow rate of 0.3mL/min. A DuoSpray Ion Source (ESI) source was used and MS spectra were acquired in positive mode in a 100 – 1000 Da mass range using external calibration. Acquisition parameters were: TEM 450, GS1 45, CUR 25, GS2 50, ISVF 5500 and DP 80. Product ion scans were acquired with CE 45 and CES 20. Data were analyzed using the PeakView v2.1 software.

5.2. General procedures of synthesis and spectral data

5.2.1 Synthesis of 2-(1,3-Benzodioxol-5-yl)ethanol (**18**)⁹

To a suspension of lithium aluminum hydride (0.114 g, 3.00 mmol) in anhydrous THF (20 mL) a solution of the acid **20** (3.00 mmol) in anhydrous THF (10 mL) was added dropwise over 15 minutes. After 4 hours, the excess of reductive agent was quenched with methanol (1 mL) and 10% aqueous NaOH solution (2 mL) until formation of aluminum hydroxide, which was neutralized with 10% aqueous hydrochloric acid solution (*ca.* 5 mL). The obtained mixture was extracted with ethyl acetate (3 x 15 mL) and the combined organic extracts were washed with brine and concentrated at reduced pressure after drying over anhydrous sodium sulfate. The residue was purified by chromatography (silica gel, CHCl₃/EtOH 100:1) to give the corresponding primary alcohol **21** as a yellow oil; 0.489 g (98%); R_f = 0.5 (CHCl₃/EtOH 20:1); IR (film, cm⁻¹) 3351, 2883, 1607, 1503, 1489, 1442, 1247, 1040; ¹H NMR (CDCl₃): δ 1.87 (br; 1H, ArCH₂CH₂OH); 2.76 (t, *J* = 6.5 Hz, 2H, ArCH₂CH₂OH); 3.78 (t, *J* = 6.5 Hz, 2H, ArCH₂CH₂OH); 5.91 (s, 2H, OCH₂O); 6.65 (dd, *J* = 7.8 Hz, *J* = 1.6 Hz, 1 H, 4'); 6.71-6.70 (m, 1H, 2'); 6.75 (d, *J* = 7.8 Hz, 1H, 5'). ¹³C NMR (CDCl₃): δ 38.6 (ArCH₂CH₂OH); 63.5 (ArCH₂CH₂OH); 100.6 (OCH₂O); 108.1 (CH, 2'); 109.1 (CH, 5'); 121.7 (CH, 6'); 132.0 (C, 1'); 145.9 (CH, 4'); 147.5 (CH, 3');

5.2.2 Synthesis of 5-(2-Bromoethyl)-1,3-benzodioxole (**12**)

To a solution of alcohol **21** (1.00 mmol) in anhydrous acetonitrile (2 mL) triphenylphosphine (0.26 g, 1.00 mmol) was added. The reaction was maintained at 0°C, while tetrabromomethane (0.33 g, 1.00 mmol) was slowly added, protected against the light, and followed by warming to room temperature, under vigorous stirring and nitrogen atmosphere for 24 hours. The solvent was then evaporated and the residue was purified by chromatography (silica gel, hexane→dichloromethane→chloroform) to give **12** as a yellow oil; 0.174 g (76%); R_f = 0.62 (CHCl₃/EtOH 20:1); IR (film, cm⁻¹) 2943, 2895, 1500, 1490, 1444, 1040; ¹H NMR (CDCl₃): δ 3.07

(t, $J = 6.0$ Hz, 2H, ArCH₂CH₂Br), 3.51 (t, $J = 6.0$ Hz, 2H, ArCH₂CH₂Br), 5.94 (s, 2H, OCH₂O), 6.67-6.76 (m, 3H, 2', 5' e 6'); ¹³C NMR (CDCl₃): δ 33.3 (ArCH₂CH₂Br), 39.1 (ArCH₂CH₂Br), 101.0 (OCH₂O), 108.4 (CH, 2'), 109.0 (CH, 5'), 121.7 (CH, 6'), 132.7 (C, 1'), 146.4 (C, 4'), 147.7 (C, 3');

5.2.3 Synthesis of 1-(2-(1,3-Benzodioxol-5-yl)ethyl)-4-(2-methoxyphenyl)piperazine (**1**)

1 was synthesized according to published procedure.⁹ R_f = 0.55 (CHCl₃/EtOH 20:1), mp 90-92 °C; IR (KBr, cm⁻¹) 3022, 2951, 2804, 1586, 1494, 1459, 1445, 1314, 1245, 1135, 1038, 752; ¹H NMR (CDCl₃): δ 2.59-2.83 (m, 8H, ArCH₂CH₂N (4H) e NCH₂CH₂NAr (4H)); 3.11-3.16 (m, 4H, NCH₂CH₂NAr); 3.75 (s, 3H, OCH₃); 5.91 (s, 2H, OCH₂O); 6.65-6.69 (m, 1H, 6'); 6.73 (m, 1H, 2'); 6.75 (d, $J = 7.7$ Hz, 1H, 5'); 6.85-6.88 (m, 1H, 6); 6.91-7.05 (m, 3H, 3, 4 e 5); ¹³C NMR (CDCl₃): δ 33.1 (ArCH₂CH₂N); 50.4 (NCH₂CH₂N); 53.1 (NCH₂CH₂N); 55.2 (ArOCH₃); 60.6 (ArCH₂CH₂N); 100.6 (OCH₂O); 108.0 (CH, 2'); 109.0 (CH, 5'); 111.0 (CH, 3); 118.0 (CH, 6); 120.8 (CH, 5); 121.2 (CH, 6'); 122.7 (CH, 4); 133.9 (C, 1'); 141.1 (C, 1); 145.6 (C, 4'); 147.3 (C, 3'); 152.1 (Ar-C, 2). HRMS (ESI) calcd for C₂₀H₂₄N₂O₃ [M + H]⁺ 341.1867, found 341.1860.

5.2.4 General procedure for the synthesis of 1-(2-alkoxyphenyl)piperazine derivatives (**2-11**)

In an Ace pressure tube, the corresponding bromide (**12-16**) (1.00 mmol), 1-phenylpiperazine derivatives (**17-19**) (1.25 mmol), triethylamine (1.25 mmol), and acetonitrile (0.5 mL) were added. The mixture was then irradiated in the microwave oven (operating at 2.45 GHz, 450 W) for 4 minutes (4 x 1'). At the end of this time the solution was concentrated in a rotatory evaporator, solubilized in dichloromethane and mixed with silica gel. The material was purified by chromatography (silica gel, dichloromethane→chloroform) to give the desired 1-(2-alkoxyphenyl)piperazine derivative.

5.2.4.1 1-(2-Methoxyphenyl)-4-phenethylpiperazine (**2,LDT2**)

Prepared by nucleophilic substitution of bromide (**13**) with 1-(2-methoxyphenyl)piperazine (**17**), as a oil; 0.275 g (93%); Rf = 0.38 (CHCl₃/EtOH 20:1); IR (film, cm⁻¹) 2942, 2808, 1594, 1500, 1309, 1240, 1026; ¹H NMR (CDCl₃): δ 2.72-2.78 (m, 2H, ArCH₂CH₂N), 2.83 (br, 4H, NCH₂CH₂N), 2.90-2.95 (m, 2H, ArCH₂CH₂N), 3.20 (br, 4H, NCH₂CH₂N), 3.88 (s, 3H, OCH₃), 6.87-6.89 (m, 1H, 6); 6.92-7.05 (m, 3H, 3, 4 e 5); 7.20-7.34 (m, 5H, 2', 3', 4', 5', 6'); ¹³C NMR (CDCl₃): δ 33.4 (ArCH₂CH₂N), 50.5 (NCH₂CH₂NAr), 53.5 (NCH₂CH₂NAr), 60.6 (ArCH₂CH₂N), 111.5 (CH, 3), 118.5 (CH, 6), 121.2 (CH, 5), 123.2 (CH, 4), 126.3 (C, 4'), 128.6 (2CH, 3', 5'), 128.9 (2CH, 2', 6'), 140.1 (C, 1'), 141.3 (C, 1), 152.5 (C, 2); HRMS (ESI) calcd for C₁₉H₂₄N₂O [M + H]⁺ 297.1969, found 297.1961.

5.2.4.2. 1-(2-(1,3-Benzodioxol-5-yl)ethyl)-4-(2-ethoxyphenyl)piperazine (**3**, LDT8)

Prepared by nucleophilic substitution of bromide (**12**) with 1-(2-ethoxyphenyl)piperazine (**18**), as a oil; 0.330 g (93%); Rf = 0.40 (CHCl₃/EtOH 20:1); IR (film, cm⁻¹) 3022, 2951, 2804, 1586, 1494, 1459, 1445, 1314, 1245, 1135, 1038, 752; ¹H NMR (CDCl₃): δ 1.46 (t, J = 6.0 Hz, 3H, ArOCH₂CH₃), 2.61-2.66 (m, 2H, ArCH₂CH₂N), 2.76-2.81 (m, 4H, NCH₂CH₂N e 2H, ArCH₂CH₂N), 3.16 (br, 4H, NCH₂CH₂N), 4.07 (q, J = 6.0 Hz, 2H, ArOCH₂CH₃), 5.92 (s, 2H, OCH₂O), 6.66-6.76 (m, 2H, 6', 2'), 6.78-6.99 (m, 5H, 5', 3, 4, 5, 6); ¹³C NMR (CDCl₃): δ HRMS (ESI) calcd for C₂₁H₂₆N₂O₃ [M + H]⁺ 355.2023, found 355.2016.

5.2.4.3. 1-(3-Methoxyphenethyl)-4-(2-ethoxyphenyl)piperazine (**4**, LDT243)

Prepared by nucleophilic substitution of bromide (**14**) with 1-(2-ethoxyphenyl)piperazine (**18**), as a white solid; 0.231 g (68%); Rf = 0.40 (CHCl₃/EtOH 20:1); mp 58-59 °C; IR (KBr, cm⁻¹) 2943, 2813, 1592, 1495, 1452, 1238, 1026; ¹H NMR (CDCl₃): δ 1.47 (t, J = 6.9 Hz, 3H, ArOCH₂CH₃), 2.73-2.94 (m, 8H, ArCH₂CH₂N, NCH₂CH₂N, ArCH₂CH₂N), 3.22 (br, 4H, NCH₂CH₂N), 3.81 (s,

3H, OCH₃), 4.08 (q, $J = 6.9$ Hz, 2H, ArOCH₂CH₃), 6.77 (dd, $J = 8.1$ Hz, $J = 2.4$ Hz, 1H, 4'), 6.81-6.87 (m, 3H, 2', 6', 6), 6.91-6.97 (m, 3H, 3, 4, 5), 7.23 (t, $J = 7.8$ Hz, 1H, 5'); ¹³C NMR (CDCl₃): δ 15.1 (ArOCH₂CH₃), 33.3 (ArCH₂CH₂N), 50.3 (NCH₂CH₂N), 53.5 (NCH₂CH₂N), 55.3 (OCH₃, 3'), 60.5 (ArCH₂CH₂N), 63.7 (ArOCH₂CH₃), 111.7 (CH, 4'), 112.7 (CH, 3), 114.7 (CH, 2'), 118.3 (CH, 6), 121.2 (CH, 5), 121.3 (CH, 6'), 123.0 (CH, 4), 129.6 (CH, 5'), 141.2 (C, 1'), 141.5 (C, 1), 151.7 (C, 2), 159.9 (C, 3'); HRMS (ESI) calcd for C₂₁H₂₈N₂O₂ [M + H]⁺ 341.2231, found 341.2224.

5.2.4.4 1-(4-Methoxyphenethyl)-4-(2-ethoxyphenyl)piperazine (**5**, LDT244)

Prepared by nucleophilic substitution of bromide (**15**) with 1-(2-ethoxyphenyl)piperazine (**18**), as a white solid; 0.286 g (84%); R_f = 0.40 (CHCl₃/EtOH 20:1); mp 48-49 °C; IR (KBr, cm⁻¹) 2973, 2947, 2814, 1609, 1589, 1307, 1245, 1044; ¹H NMR (CDCl₃): δ 1.47 (t, $J = 6.8$ Hz, 3H, ArOCH₂CH₃), 2.67-2.70 (m, 2H, ArCH₂CH₂N), 2.79 (br, 4H, NCH₂CH₂N), 2.83-2.86 (m, 2H, ArCH₂CH₂N), 3.20 (br, 4H, NCH₂CH₂N), 3.80 (s, 3H, OCH₃), 4.08 (q, $J = 6.8$ Hz, 2H, ArOCH₂CH₃), 6.85-6.86 (m, 3H, 3', 5', 6), 6.91-6.99 (m, 3H, 3, 4, 5), 7.16 (d, $J = 8.2$ Hz, 2H, 2', 6'). ¹³C NMR (CDCl₃): δ 15.1 (ArOCH₂CH₃), 32.6 (ArCH₂CH₂N), 50.5 (NCH₂CH₂N), 53.5 (NCH₂CH₂N), 55.4 (OCH₃, 4'), 60.9 (ArCH₂CH₂N), 63.7 (ArOCH₂CH₃), 112.6 (CH, 3), 114.0 (2CH, 3', 5'), 118.3 (CH, 6), 121.1 (CH, 5), 122.9 (CH, 4), 129.8 (2CH, 2', 6'), 132.3 (C, 1'), 141.4 (C, 1), 151.7 (C, 2), 158.1 (C, 4'); HRMS (ESI) calcd for C₂₁H₂₈N₂O₂ [M + H]⁺ 341.2231, found 341.2224.

5.2.4.5 1-(3,4-Dimethoxyphenethyl)-4-(2-ethoxyphenyl)piperazine (**6**, LDT245)

Prepared by nucleophilic substitution of bromide (**16**) with 1-(2-ethoxyphenyl)piperazine (**18**), as an oil; 0.256 g (69%); R_f = 0.40 (CHCl₃/EtOH 20:1); IR (film, cm⁻¹) 2927, 2827, 1609, 1582, 1304, 1241, 1028; ¹H NMR (CDCl₃): δ 1.48 (t, 3H, $J = 6.93$ Hz, ArOCH₂CH₃), 2.68-2.73 (m, 2H, ArCH₂CH₂N), 2.77 (br, 4H, NCH₂CH₂N), 2.82-2.89 (m, 2H, ArCH₂CH₂N), 3.19 (br, 4H, NCH₂CH₂N), 3.81 (s, 3H, OCH₃), 3.81 (s, 3H, OCH₃), 4.09 (q, $J = 6.90$ Hz, 2H, ArOCH₂CH₃),

6.75-6.83 (m, 3H, 3', 5', 6), 6.83-6.92 (d, $J = 6.0$ Hz, 1H, 6'), 6.92-6.99 (m, 3H, 3, 4, 5); ^{13}C NMR (CDCl_3): δ 15.0 ($\text{ArOCH}_2\text{CH}_3$), 33.7 ($\text{ArCH}_2\text{CH}_2\text{N}$), 50.6 ($\text{NCH}_2\text{CH}_2\text{N}$), 53.6 ($\text{NCH}_2\text{CH}_2\text{N}$), 55.2 (OCH_3 , 3'), 55.2 (OCH_3 , 4'), 60.5 ($\text{ArCH}_2\text{CH}_2\text{N}$), 63.7 ($\text{ArOCH}_2\text{CH}_3$), 111.4 (CH , 3), 112.7 (CH , 5'), 114.6 (CH , 2'), 118.3 (CH , 6), 120.1 (CH , 6'), 121.2 (CH , 5), 122.8 (CH , 4), 129.5 (C , 1), 141.5 (C , 1), 142.0 (C , 4'), 151.7 (C , 3'), 159.8 (C , 2); HRMS (ESI) calcd for $\text{C}_{22}\text{H}_{30}\text{N}_2\text{O}_3$ [$\text{M} + \text{H}$] $^+$ 371.2336, found 371.2329.

5.2.4.6 1-(2-(1,3-Benzodioxol-5-yl)ethyl)-4-(2-isopropoxyphenyl)piperazine (7, LDT451)

Prepared by nucleophilic substitution of bromide (**12**) with 1-(2-isopropoxyphenyl)piperazine (**19**), as a white solid; 0.295 g (80%); $R_f = 0.43$ ($\text{CHCl}_3/\text{EtOH}$ 20:1); mp 59-60 °C; IR (KBr, cm^{-1}) 2974, 2941, 2816, 1595, 1492, 1382, 1317, 1311, 1122, 1008; ^1H NMR (CDCl_3): δ 1.37 (d, $J = 6.0$ Hz, 6H, $\text{ArOCH}(\text{CH}_3)_2$), 2.62-2.68 (m, 2H, $\text{ArCH}_2\text{CH}_2\text{N}$, 4H, $\text{NCH}_2\text{CH}_2\text{N}$ e 2H, $\text{ArCH}_2\text{CH}_2\text{N}$), 3.17 (br, 4H, $\text{NCH}_2\text{CH}_2\text{N}$), 4.61 (hp, $J = 6.0$ Hz, 1H, $\text{ArOCH}(\text{CH}_3)_2$), 5.92 (s, 2H, OCH_2O), 6.67-6.70 (m, 1H, 6'), 6.67-6.77 (m, 2H, 2', 5'), 6.84-6.91 (m, 1H, 6), 6.92-6.98 (m, 3H, 3, 4, 5); ^{13}C NMR (CDCl_3): δ 22.5 ($\text{ArOCH}(\text{CH}_3)_2$), 33.4 ($\text{ArCH}_2\text{CH}_2\text{N}$), 50.5 ($\text{NCH}_2\text{CH}_2\text{N}$), 53.7 ($\text{NCH}_2\text{CH}_2\text{N}$), 60.9 ($\text{ArCH}_2\text{CH}_2\text{N}$), 70.4 ($\text{ArOCH}(\text{CH}_3)_2$), 100.9 (OCH_2O), 108.2 (CH , 2'), 109.3 (CH , 5'), 116.4 (CH , 3), 118.7 (CH , 6), 121.6 (2CH , 5, 6'), 122.6 (CH , 4), 134.0 (C , 1'), 142.9 (C , 1), 145.9 (C , 4'), 147.7 (C , 3'), 150.6 (C , 2); HRMS (ESI) calcd for $\text{C}_{22}\text{H}_{28}\text{N}_2\text{O}_3$ [$\text{M} + \text{H}$] $^+$ 369.2180, found 369.2173.

5.2.4.7 1-(2-Isopropoxyphenyl)-4-phenethylpiperazine (8, LDT452)

Prepared by nucleophilic substitution of bromide (**13**) with 1-(2-isopropoxyphenyl)piperazine (**19**), as a white solid; 0.266 g (82%); $R_f = 0.38$ ($\text{CHCl}_3/\text{EtOH}$ 20:1); mp 67-68 °C; IR (KBr, cm^{-1}) 2975,

2943, 2811, 1592, 1495, 1382, 1371, 1237, 1128, 1040; ^1H NMR (CDCl_3): δ 1.38 (d, $J = 10.0$ Hz, 6H, $\text{ArOCH}(\text{CH}_3)_2$), 2.68-2.75 (m, 2H, $\text{ArCH}_2\text{CH}_2\text{N}$ e 4H, $\text{NCH}_2\text{CH}_2\text{N}$), 2.85-2.98 (m, 2H, $\text{ArCH}_2\text{CH}_2\text{N}$), 3.19 (br, 4H, $\text{NCH}_2\text{CH}_2\text{N}$), 4.62 (hp, $J = 10.0$ Hz, 1H, $\text{ArOCH}(\text{CH}_3)_2$), 6.88-6.90 (m, 1H, 6), 6.89-6.98 (m, 3H, 3, 4, 5), 7.20-7.34 (m, 5H, 2', 3', 4', 5', 6'); ^{13}C NMR (CDCl_3): δ 22.4 ($\text{ArOCH}(\text{CH}_3)_2$), 33.7 ($\text{ArCH}_2\text{CH}_2\text{N}$), 50.5 ($\text{NCH}_2\text{CH}_2\text{NAr}$), 53.7 ($\text{NCH}_2\text{CH}_2\text{NAr}$), 60.7 ($\text{ArCH}_2\text{CH}_2\text{N}$), 70.4 ($\text{ArOCH}(\text{CH}_3)_2$), 116.3 (CH , 3), 118.6 (CH , 6), 121.6 (CH , 5), 122.7 (CH , 4), 126.2 (C , 4'), 128.6 (2 CH , 3', 5'), 128.9 (2 CH , 2', 6'), 140.0 (C , 1'), 142.3 (C , 1), 150.5 (C , 2); HRMS (ESI) calcd for $\text{C}_{21}\text{H}_{28}\text{N}_2\text{O}$ [$\text{M} + \text{H}$] $^+$ 325.2282, found 326.2274.

5.2.4.8 1-(3-Methoxyphenethyl)-4-(2-isopropoxyphenyl)piperazine (**9**, LDT453)

Prepared by nucleophilic substitution of bromide (**14**) with 1-(2-isopropoxyphenyl)piperazine (**19**), as a white solid; 0.142 g (40%); $R_f = 0.42$ ($\text{CHCl}_3/\text{EtOH}$ 20:1); mp 57-58 °C; IR (KBr, cm^{-1}) 2944, 2809, 1583, 1492, 1444, 1370, 1311, 1236, 1125, 1054; ^1H NMR (CDCl_3): δ 1.37 (d, $J = 6.0$ Hz, 6H, $\text{ArOCH}(\text{CH}_3)_2$), 2.71-2.75 (m, 2H, $\text{ArCH}_2\text{CH}_2\text{N}$), 2.78 (br, 4H, $\text{NCH}_2\text{CH}_2\text{N}$), 2.87-2.91 (m, 2H, $\text{ArCH}_2\text{CH}_2\text{N}$), 3.20 (br, 4H, $\text{NCH}_2\text{CH}_2\text{N}$), 3.81 (s, 3H, OCH_3), 4.61 (hp, $J = 6.0$ Hz, 1H, $\text{ArOCH}(\text{CH}_3)_2$), 6.77 (dd, $J = 8.1$ Hz, $J = 2.0$ Hz, 1H, 4'), 6.81 (br, 1H, 2'), 6.84 (d, $J = 7.5$ Hz, 1H, 6'), 6.88 (d, $J = 7.2$ Hz, 1H, 6), 6.91-6.97 (m, 3H, 3, 4, 5), 7.23 (t, $J = 7.8$ Hz, 1H, 5'); ^{13}C NMR (CDCl_3): δ 22.5 ($\text{ArOCH}(\text{CH}_3)_2$), 33.5 ($\text{ArCH}_2\text{CH}_2\text{N}$), 50.3 ($\text{NCH}_2\text{CH}_2\text{N}$), 53.6 ($\text{NCH}_2\text{CH}_2\text{N}$), 55.3 (OCH_3 , 3'), 60.5 ($\text{ArCH}_2\text{CH}_2\text{N}$), 70.4 ($\text{ArOCH}(\text{CH}_3)_2$), 111.6 (CH , 4'), 114.7 (CH , 2'), 116.1 (CH , 3), 118.7 (CH , 6), 121.3 (CH , 5), 121.6 (CH , 6'), 122.7 (CH , 4), 129.6 (CH , 5'), 142.0 (C , 1'), 143.0 (C , 1), 150.5 (C , 2), 159.9 (C , 3'); HRMS (ESI) calcd for $\text{C}_{22}\text{H}_{30}\text{N}_2\text{O}_2$ [$\text{M} + \text{H}$] $^+$ 355.2387, found 355.2380.

5.2.4.9 1-(4-Methoxyphenethyl)-4-(2-isopropoxyphenyl)piperazine (**10**, LDT454)

Prepared by nucleophilic substitution of bromide (**15**) with 1-(2-isopropoxyphenyl)piperazine (**19**), as an oil; 0.184 g (52%); $R_f = 0.42$ ($\text{CHCl}_3/\text{EtOH}$ 20:1); IR (film, cm^{-1}) 2973, 2936, 2812, 1610, 1595, 1512, 1496, 1372, 1300, 1239, 1134, 1039; ^1H NMR (CDCl_3): δ 1.37 (d, $J = 6.0$ Hz, 6H,

ArOCH(CH₃)₂), 2.66-2.69 (m, 2H, ArCH₂CH₂N), 2.76 (br, 4H, NCH₂CH₂N), 2.82-2.86 (m, 2H, ArCH₂CH₂N), 3.19 (br, 4H, NCH₂CH₂N), 3.80 (s, 3H, OCH₃), 4.62 (hp, *J* = 6.0 Hz, 1H, ArOCH(CH₃)₂), 6.85-6.89 (m, 3H, *J* = 8.4 Hz, 3', 5', 6), 6.94-6.95 (m, 3H, 3, 4, 5), 7.16 (d, *J* = 8.4 Hz, 2H, 2', 6'); ¹³C NMR (CDCl₃): δ 22.5 (ArOCH(CH₃)₂), 33.7 (ArCH₂CH₂N), 50.5 (NCH₂CH₂N), 53.7 (NCH₂CH₂N), 55.4 (OCH₃, 4'), 60.9 (ArCH₂CH₂N), 70.5 (ArOCH(CH₃)₂), 114.1 (2CH, 3', 5'), 116.4 (CH, 3), 118.7 (CH, 6), 121.7 (CH, 5), 122.7 (CH, 4), 129.8 (2CH, 2', 6'), 132.4 (C, 1'), 142.9 (C, 1), 150.6 (C, 2), 158.2 (C, 4'); HRMS (ESI) calcd for C₂₂H₃₀N₂O₂ [M + H]⁺ 355.2387, found 355.2380.

5.2.4.10 1-(3,4-Dimethoxyphenethyl)-4-(2-isopropoxyphenyl)piperazine (**11**, LDT455)

Prepared by nucleophilic substitution of bromide (**16**) with 1-(2-isopropoxyphenyl)piperazine (**19**), as an oil; 0.212 g (55%); R_f = 0.45 (CHCl₃/EtOH 20:1); IR (film, cm⁻¹) 2972, 2936, 2812, 1592, 1516, 1497, 1354, 1372, 1237, 1141, 1030; ¹H NMR (CDCl₃): δ 1.36 (d, *J* = 6.0 Hz, 6H, ArOCH(CH₃)₂), 2.68-2.71 (m, 2H, ArCH₂CH₂N), 2.76 (br, 4H, NCH₂CH₂N), 2.82-2.87 (m, 2H, ArCH₂CH₂N), 3.19 (br, 4H, NCH₂CH₂N), 3.86 (s, 3H, OCH₃), 3.88 (s, 3H, OCH₃), 4.60 (hp, *J* = 6.0 Hz, 1H, ArOCH(CH₃)₂), 6.77-6.82 (m, 3H, 2', 5', 6), 6.86-6.88 (m, 1H, 6'), 6.93-6.95 (m, 3H, 3, 4, 5); ¹³C NMR (CDCl₃): δ 22.5 (ArOCH(CH₃)₂), 33.2 (ArCH₂CH₂N), 50.4 (NCH₂CH₂N), 53.7 (NCH₂CH₂N), 56.0 (OCH₃, 4'), 56.1 (OCH₃, 3'), 60.9 (ArCH₂CH₂N), 70.5 (ArOCH(CH₃)₂), 111.6 (CH, 5'), 112.4 (CH, 2'), 116.4 (CH, 3), 118.7 (CH, 6), 120.7 (CH, 6'), 121.7 (CH, 5), 122.7 (CH, 4), 132.9 (C, 1'), 142.9 (C, 1), 147.5 (C, 4'), 149.0 (C, 3), 151.7 (C, 2); HRMS (ESI) calcd for C₂₃H₃₂N₂O₃ [M + H]⁺ 385.2493, found 385.2486.

5.3. Biology

5.3.1. Binding assays

Competition binding assays to cloned human α_{1a}, α_{1b}, and α_{1d}-adrenoceptor subtypes were performed in membrane preparations from CHO (Chinese Hamster Ovary) cell lines transfected by electroporation with DNA expressing the gene encoding each α₁-adrenoceptor. Cloning and stable

expression of the human α_1 -adrenoceptor gene was performed as previously described.²² Briefly, CHO cells membranes (30 μ g proteins) were incubated in 50 mM Tris-HCl buffer, pH 7.4, with 0.1–0.4 nM [³H]prazosin, in a final volume of 1.02 mL for 30 min at 25 °C, in the absence or presence of competing drugs (1 pM–10 μ M). Non-specific binding was determined in the presence of 10 μ M phentolamine. The incubation was stopped by addition of ice-cold Tris-HCl buffer and rapid filtration through 0.2% poly(ethylenimine)-pretreated Whatman GF/B or Schleicher & Schuell GF52 filters.

5.3.2 Functional experiments

Male Wistar rats (275–300 g) were killed by cervical dislocation and the required organs were isolated, freed from adhering connective tissue, and set up rapidly under a suitable resting tension in 20 mL organ baths containing physiological salt solution kept at 37 °C and aerated with 5% CO₂:95% O₂ at pH 7.4. Concentration-response curves were constructed by cumulative addition of reference agonist. The concentration of agonist in the organ bath was increased approximately 3-fold at each step, with each addition being made only after the response to the previous addition had attained a maximal level and remained steady. Contractions were recorded by means of a transducer connected to the MacLab system PowerLab/800. At first the compounds under study were added in the organ bath in order to construct a concentration response curve such as that for the reference agonist, but no response was obtained; after this, the compounds were treated as antagonists. In particular, after construction of concentration-response curves of the reference agonist following 30 min of washing, tissues were incubated with the compound under study for 30 min and a new concentration-response curve to the agonist was recorded. In all cases, parallel experiments in which tissues received only the reference agonist were run in order to check any variation in sensitivity.

All animal testing was carried out according to European Communities Council Directive of 24 November 1986 (86/609/EEC).

The antagonist potency was expressed by pK_B at a single concentration²³ or pA_2 when indicated.¹⁴,¹⁸ pK_B values were calculated from the equation $pK_B = \log(DR - 1) - \log[B]$, where DR is the ratio of ED_{50} values of agonist after and before treatment with one or two antagonist concentrations [B]. pA_2 was calculated from Schild plot constraining the slope to -1. Data are presented as the mean \pm SE of 4-5 experiments. Differences between mean values were tested for significance by Student's t-test.

5.3.2.1 Rat vas deferens prostatic portion

This tissue was used to assess $\alpha 1A$ -AR antagonism.²⁴ Prostatic portions of 2-cm length were mounted under 0.35 g tension at 37 °C in a Tyrode solution of the following composition (mM): NaCl, 130; KCl, 2; CaCl₂, 1.8; MgCl₂, 0.89; NaH₂PO₄, 0.42; NaHCO₃, 25; glucose, 5.6. Cocaine hydrochloride (10 mM) was added to the Tyrode to prevent the neuronal uptake of (-)-NE. After the equilibration period, tissues were primed twice by addition of 10 μ M of the agonist (-)-NE in order to obtain a constant response. After another washing and equilibration period of 45 min, a cumulative (-)-NE concentration-response curve was constructed isotonicly to determine the relationship between agonist concentrations and the contractile response (basal response). When measuring the effect of the antagonist, it was allowed to equilibrate with the tissue for 60 min before constructing a new concentration-response curve to the agonist. (-)-NE solution contained 0.05% Na₂S₂O₅ to prevent oxidation.

5.3.2.2 Rat spleen

This tissue was used to assess $\alpha 1B$ -AR antagonism.²⁵ The spleen was removed and bisected longitudinally into two strips which were suspended in tissue baths containing Krebs solution of the following composition (mM): NaCl, 120; KCl, 4.7; CaCl₂, 2.5; MgSO₄, 1.5; KH₂PO₄, 1.2; NaHCO₃, 20; glucose, 11; K₂EDTA, 0.01. (\pm)-Propranolol hydrochloride (4 μ M) was added to

block β -adrenoceptors. The spleen strips were placed under 1 g resting tension and equilibrated for 2 h. The cumulative concentration-response curves to phenylephrine were measured isometrically and obtained at 30 min intervals, the first one being discarded and the second one taken as control. The antagonist was allowed to equilibrate with the tissue for 30 min; then a new concentration-response curve to the agonist was constructed.

5.3.2.3 Rat aorta

This tissue was used to assess α 1D-AR antagonism.¹⁴ Thoracic aorta was cleaned from extraneous connective tissue and placed in Krebs solution of the following composition (mM): NaCl, 118.4; KCl, 4.7; CaCl₂, 1.9; MgSO₄, 1.2; NaH₂PO₄, 1.2; NaHCO₃, 25; glucose, 11.7. Cocaine hydrochloride (10 μ M), normetanephrine hydrochloride (1 μ M) and (\pm)-propranolol hydrochloride (1 μ M) were added to prevent the neuronal and extraneuronal uptake of (-)-NE and to block β -adrenoceptors, respectively. Two helicoidal strips (15 x 3 mm) were cut from each aorta beginning from the end most proximal to the heart. The endothelium was removed by rubbing with filter paper: the absence of acetylcholine (100 μ M)-induced relaxation to preparations contracted with (-)-NE (1 μ M) was taken as an indicator that vessel was denuded successfully. Vascular strips were then tied with surgical thread and suspended in a jacketed tissue bath containing Krebs solution. Strip contractions were measured isometrically. After at least a 2 h equilibration period under an optimal tension of 1 g, cumulative (-)-NE concentration-response curves were recorded at 1 h intervals, the first two being discarded and the third one taken as a control. The antagonist was allowed to equilibrate with the tissue for 60 min before the generation of the fourth cumulative concentration-response curve to (-)-NE. (-)-NE solutions contained 0.05% Na₂S₂O₄ to prevent oxidation.

5.3.3 Cellular studies

Caucasian prostate adenocarcinoma PC-3 cell line was used to study compound **7**'s antiproliferative activity. This cell line was grown adherently and maintained in minimum essential medium supplemented with 100 U/mL penicillin, 100 $\mu\text{g}/\text{mL}$ streptomycin, and 10% fetal bovine serum (FBS) and cultured at 37° C and aerated with 5% CO₂ : 95% O₂.

Tested compound was dissolved in methanol (MeOH) at a concentration of 10.000 μM and diluted with specific cells medium prior to use. Ten thousand cells were suspended in 98 μL of specific medium and incubated in a 96-well plate for overnight. After the incubation, 2 μL of understudy compound was added to the well with the final concentrations of 0.01 to 10 μM . After 24, 48, and 72 h incubation at 37 °C, viability of the cells was determined by 3-(4,5-dimethylthiazol-2-yl)-5-(3-carboxymethoxyphenyl)- 2-(4-sulfenyl)-2H-tetrazolium (MTS) assay using Cell Titer 96 Aqueous One Solution Cell Proliferation Assay (Promega Italia Srl).²⁶ After the addition of MTS, in combination with the electron coupling agent phenazine methosulfate, the cells were allowed to incubate for 1 h and absorbance was measured at 492 nm in a microplate reader, GeniosPro. Cell viability was calculated as a percentage using the formula: (mean OD of treated cells/mean OD of control cells) \times 100. Results are expressed as percent of control cells which are not treated. The growth control (GC) and growth control with MeOH (GCM) were run for each set of cell line. All experiments were done in triplicate.

5.4. Docking studies

The primary sequences of the three α 1-AR subtypes were retrieved from UniProt (ID: α 1a = P35348, ADA1A_HUMAN; α 1b = P35368, ADA1B_HUMAN; α 1d = P25100, ADA1D_HUMAN) and the homology models were generated by using Modeller 9.15²⁷ based on the resolved structure of human β 2-adrenergic receptor (PDB Id: 2RH1). Among the 10 produced models, the best structure was chosen by considering the DOPE and GA341 scoring functions as well as some well-known structural parameters such as the percentages of residues falling in the allowed regions of the Ramachandran plot and the chi-space. For all considered subtypes, the

selected models did not include the large intracellular C-terminal domains, which indeed is not involved in the binding pocket (excluded residues: 330-446 for a1a, 352-520 for a1b and 406-572 for a1d). After a set of geometrical checks to avoid unphysical occurrences such as unpredicted gaps, incorrect D-residues, cis peptide bonds, colliding side-chains or unsuitable bond lengths, the selected models were optimized by energy minimization keeping fixed the backbone atoms to preserve the predicted folding.

The ligands were simulated in their protonated state since this is involved in receptor binding. Their conformational profile was explored by quenched MonteCarlo simulations (as implemented in the VEGA program,²⁸ which produced 1000 minimized conformations by randomly rotating the rotatable bonds and the so computed lowest energy conformers underwent docking simulations. Docking analyses were carried out by using Plants, which calculates reliable ligand poses by ant colony organization algorithms.²⁹ For all receptor models, the search was focused into a 8 Å radius sphere around the key aspartate residue, namely Asp106 or a1a, Asp125 for a1b and Asp176 for a1d. 10 poses were generated for each ligand and scored by the Plp95 function with a speed equal to 1. The obtained best complexes were finally minimized by keeping fixed all atoms outside a 8 Å radius sphere around the bound ligand and the so optimized complexes were utilized to recalculate the docking scores.

Acknowledgments

ERS and LASR are senior fellow of the National Counsel of Technological and Scientific Development (CNPq #310509/2011-4, Brazil). This work was supported by CNPq #473053/2004-7 grant to LASR. MLB is supported by a grant of Visiting Professor (PVE – CNPq#401864/2013-8) from the programme “Ciência sem Fronteiras”, Brazil.

References

1. Ruffolo, R. R.; Hieble, J. P., Adrenoceptor pharmacology: Urogenital applications. *Eur Urol* **1999**, *36*, 17-22.
2. Rosini, M.; Bolognesi, M. L.; Giardina, D.; Minarini, A.; Tumiatti, V.; Melchiorre, C., Recent advances in alpha1-adrenoreceptor antagonists as pharmacological tools and therapeutic agents. *Curr. Top. Med. Chem.* **2007**, *7* (2), 147-62.
3. Cotecchia, S., The alpha1-adrenergic receptors: diversity of signaling networks and regulation. *J. Recept. Signal Transduc. Res.* **2010**, *30* (6), 410-9.
4. Kumar, R.; Malla, P.; Kumar, M., Advances in the design and discovery of drugs for the treatment of prostatic hyperplasia. *Expert Opin. Drug. Disc.* **2013**, *8* (8), 1013-1027.
5. Lepor, H.; Kazzazi, A.; Djavan, B., alpha-Blockers for benign prostatic hyperplasia: the new era. *Curr. Opin. Urol.* **2012**, *22* (1), 7-15.
6. Dunn, C. J.; Matheson, A.; Faulds, D. M., Tamsulosin - A review of its pharmacology and therapeutic efficacy in the management of lower urinary tract symptoms. *Drug Aging* **2002**, *19* (2), 135-161.
7. Russo, A.; La Croce, G.; Capogrosso, P.; Ventimiglia, E.; Colicchia, M.; Serino, A.; Mirone, V.; Damiano, R.; Montorsi, F.; Salonia, A., Latest pharmacotherapy options for benign prostatic hyperplasia. *Expert Opin. Pharmacol.* **2014**, *15* (16), 2319-2328.
8. Zhang, W.; Ma, Z.; Li, W. H.; Li, G.; Chen, L. Z.; Liu, Z. Z.; Du, L. P.; Li, M. Y., Discovery of Quinazoline-Based Fluorescent Probes to alpha(1)-Adrenergic Receptors. *ACS Med. Chem. Lett.* **2015**, *6* (5), 502-506.
9. Romeiro, L. A.; da Silva Ferreira, M.; da Silva, L. L.; Castro, H. C.; Miranda, A. L.; Silva, C. L.; Noel, F.; Nascimento, J. B.; Araujo, C. V.; Tibirica, E.; Barreiro, E. J.; Fraga, C. A., Discovery of LASSBio-772, a 1,3-benzodioxole N-phenylpiperazine derivative with potent alpha 1A/D-adrenergic receptor blocking properties. *Eur. J. Med. Chem.* **2011**, *46* (7), 3000-12.
10. Chagas-Silva, F.; Nascimento-Viana, J. B.; Romeiro, L. A.; Barberato, L. C.; Noel, F.; Silva, C. L., Pharmacological characterization of N1-(2-methoxyphenyl)-N4-hexylpiperazine as a multi-target antagonist of alpha1A/alpha1D-adrenoceptors and 5-HT1A receptors that blocks prostate contraction and cell growth. *Naunyn-Schmiedeberg's Arch. Pharmacol.* **2014**, *387* (3), 225-34.
11. Kuo, G. H.; Prouty, C.; Murray, W. V.; Pulito, V.; Jolliffe, L.; Cheung, P.; Varga, S.; Evangelisto, M.; Wang, J., Design, synthesis, and structure-activity relationships of phthalimide-phenylpiperazines: a novel series of potent and selective alpha(1)(a)-adrenergic receptor antagonists. *J. Med. Chem.* **2000**, *43* (11), 2183-95;
12. Khatuya, H.; Hutchings, R. H.; Kuo, G. H.; Pulito, V. L.; Jolliffe, L. K.; Li, X.; Murray, W. V., Arylpiperazine substituted heterocycles as selective alpha(1a) adrenergic antagonists. *Bioorg. Med. Chem. Lett.* **2002**, *12* (17), 2443-6.
13. Richardson, T. I.; Ornstein, P. L.; Briner, K.; Fisher, M. J.; Backer, R. T.; Biggers, C. K.; Clay, M. P.; Emmerson, P. J.; Hertel, L. W.; Hsiung, H. M.; Husain, S.; Kahl, S. D.; Lee, J. A.; Lindstrom, T. D.; Martinelli, M. J.; Mayer, J. P.; Mullaney, J. T.; O'Brien, T. P.; Pawlak, J. M.; Revell, K. D.; Shah, J.; Zgombick, J. M.; Herr, R. J.; Melekhov, A.; Sampson, P. B.; King, C. H., Synthesis and structure-activity relationships of novel arylpiperazines as potent and selective agonists of the melanocortin subtype-4 receptor. *J. Med. Chem.* **2004**, *47* (3), 744-55.
14. Sagratini, G.; Angeli, P.; Buccioni, M.; Gulini, U.; Marucci, G.; Melchiorre, C.; Poggesi, E.; Giardina, D., Synthesis and alpha1-adrenoceptor antagonist activity of tamsulosin analogues. *Eur. J. Med. Chem.* **2010**, *45* (12), 5800-5807.
15. Filippi, S.; Parenti, A.; Donnini, S.; Granger, H. J.; Fazzini, A.; Ledda, F., alpha(1D)-adrenoceptors cause endothelium-dependent vasodilatation in the rat mesenteric vascular bed. *J. Pharmacol. Exp. Ther.* **2001**, *296* (3), 869-75.
16. Antonello, A.; Hrelia, P.; Leonardi, A.; Marucci, G.; Rosini, M.; Tarozzi, A.; Tumiatti, V.; Melchiorre, C., Design, synthesis, and biological evaluation of prazosin-related derivatives as multipotent compounds. *J. Med. Chem.* **2005**, *48* (1), 28-31.

17. Kenakin, T., Quantifying Biological Activity in Chemical Terms: A Pharmacology Primer To Describe Drug Effect. *ACS Chem. Biol.* **2009**, *4* (4), 249-260.
18. Scapecchi, S.; Nesi M.; Matucci, R.; Bellucci, C.; Buccioni, M.; Dei, S.; Guandalini, L.; Manetti, D.; Martelli, C.; Martini, E.; Marucci, G.; Orlandi, F.; Romanelli, M.N.; Teodori, E.; Cirilli, R. Synthesis, Affinity Profile and Functional Activity of Potent Chiral Muscarinic Antagonists with a Pyrrolidinylfuran Structure. *J. Med. Chem.*, **2010**, *53* (1), 201–207.
19. Maïga, A.; Dupont, M.; Blanchet, G.; Marcon, E.; Gilquin, B.; Servent, D.; Gilles, N. Molecular exploration of the $\alpha(1A)$ -adrenoceptor orthosteric site: binding site definition for epinephrine, HEAT and prazosin. *FEBS Lett.* **2014**, *588*, 4613-4619.
20. Kyprianou, N. Benning, C. M., Suppression of Human Prostate Cancer Cell Growth By $\alpha 1$ -Adrenoceptor Antagonists Doxazosin and Terazosin via Induction of Apoptosis. *Cancer Res.* **2000**, *60*, 4550-4555.
21. Nascimento-Viana, J. B.; Carvalho, A. R.; Nasciutti, L. E.; Alcántara-Hernández, R.; Chagas-Silva, F.; Souza, P. A. R.; Romeiro, L. A.; García-Sáinz, J. A.; Noel, F.; Silva, C. L., New high-affinity antagonists of $\alpha 1A$ -/ $\alpha 1D$ -adrenoceptors and 5-1 HT1A receptors are potential lead compounds for multi-targeted therapy against benign prostatic hyperplasia. *J. Pharmacol. Exp. Ther.* **2016**, *356* (1), 212-222.
22. Testa, R.; Guarneri, L.; Angelico, P.; Poggesi, E.; Taddei, C.; Sironi, G.; Colombo, D.; Sulpizio, A. C.; Naselsky, D. P.; Hieble, J. P.; Leonardi, A., Pharmacological characterization of the uroselective alpha-1 antagonist Rec 15/2739 (SB 216469): role of the alpha-1L adrenoceptor in tissue selectivity, part II. *J. Pharmacol. Exp. Ther.* **1997**, *281* (3), 1284-93.
23. Romeo, G.; Salerno, L.; Pittala, V.; Modica, M. N.; Siracusa, M. A.; Materia, L.; Buccioni, M.; Marucci, G.; Minneman, K. P., High affinity ligands and potent antagonists for the alpha1D-adrenergic receptor. Novel 3,8-disubstituted [1]benzothieno[3,2-d]pyrimidine derivatives. *Eur. J. Med. Chem.* **2014**, *83*, 419-32.
24. Buccioni, M.; Kandhavelu, M.; Angeli, P.; Cristalli, G.; Dal Ben, D.; Giardina, D.; Lambertucci, C.; Lammi, C.; Volpini, R.; Marucci, G., Identification of alpha1-adrenoceptor subtypes involved in contraction of young CD rat epididymal vas deferens. *Eur. J. Pharmacol.* **2009**, *602* (2-3), 388-94.21.
25. Prandi, A.; Franchini, S.; Manasieva, L. I.; Fossa, P.; Cichero, E.; Marucci, G.; Buccioni, M.; Cilia, A.; Pirona, L.; Brasili, L., Synthesis, biological evaluation, and docking studies of tetrahydrofuran- cyclopentanone- and cyclopentanol-based ligands acting at adrenergic alpha(1)- and serotoninine 5-HT1A receptors. *J. Med. Chem.* **2012**, *55* (1), 23-36.
26. Buccioni, M.; Dal Ben, D.; Lambertucci, C.; Maggi, F.; Papa, F.; Thomas, A.; Santinelli, C.; Marucci, G. Antiproliferative Evaluation of Isofuranodiene on Breast and Prostate Cancer Cell Lines. *Sci. World J.* **2014**, ID 264829, 6p
27. Marti-Renom, M. A.; Stuart A.; Fiser, A., Sánchez, R.; Melo, F.; Sali., A., Comparative protein structure modeling of genes and genomes. *Annu. Rev. Biophys. Biomol. Struct.* **2000**, *29*, 291-325.
28. Pedretti A.; Villa L.; Vistoli G., VEGA: a versatile program to convert, handle and visualize molecular structure on Windows-based PCs. *J. Mol. Graph. Model.* **2002**, *21*, 47-49.
29. Korb, O.; Stütze, T.; Exner, T. E., Empirical Scoring Functions for Advanced Protein-Ligand Docking with PLANTS. *J. Chem. Inf. Model.* **2009**, *49*, 84-96.

Table 1. Binding affinity constants of target compounds **2-11** and reference compounds **1** and tamsulosin, at cloned human α_1 -AR subtypes expressed in CHO cells.

Compounds		pK_i , ^a			Selectivity ^b		
N ^o	Code	α_{1a}	α_{1b}	α_{1d}	α_{1d}/α_{1a}	α_{1d}/α_{1b}	α_{1a}/α_{1b}
1	LASSBio 772	8.46	8.28	8.90	2.5	4.0	1.5
2	LDT2	7.50	7.04	7.78	2.0	5.5	3.0
3	LDT8	8.95	8.27	8.82	0.5	3.5	5.0
4	LDT243	8.53	7.60	8.59	1.0	9.5	8.5
5	LDT244	8.95	7.99	8.87	1.0	7.5	9.0
6	LDT245	8.68	7.80	9.22	3.5	26	7.5
7	LDT451	9.41	7.89	8.76	0.2	7.5	32
8	LDT452	8.30	7.11	8.34	1.0	17	15
9	LDT453	8.56	7.86	8.88	2.0	10	5
10	LDT454	8.65	7.83	8.51	0.5	4.5	6.5
11	LDT455	8.70	7.98	8.87	1.5	7.5	5.0
Tamsulosin		10.30 ^c	9.20 ^c	10.00 ^c	0.5	6.0	13

^a Log equilibrium dissociation constants (pK_i) were calculated from IC_{50} values using the Cheng–Prusoff equation. The affinity estimates, derived from displacement of [³H]prazosin binding from α_1 -adrenoceptors and expressed as mean values, were from two to three experiments performed in triplicate, which agreed within $\pm 20\%$.

^b Calculated by the antilog of the difference between pK_i values at different α_1 -adrenoceptor subtypes.

^c Data from ref 14.

Table 2. Antagonist potency of target compounds **2-11** and reference compounds **1** and tamsulosin in isolated rat prostatic vas deferens (α_{1A} -AR), spleen (α_{1B} -AR) and thoracic aorta (α_{1D} -AR).

Compounds		pK_B^a			Selectivity ^b		
No	Code	α_{1A} rat vas deferens	α_{1B} rat spleen	α_{1D} rat aorta	α_{1D}/α_{1A}	α_{1D}/α_{1B}	α_{1A}/α_{1B}
1	LASSBio 772	8.47 ± 0.09	8.11 ± 0.02	8.57 ± 0.02	1	3	2
2	LDT2	7.76 ± 0.16	7.82 ± 0.13	8.50 ± 0.07	5	5	1
3	LDT8	9.09 ± 0.08	8.85 ± 0.14	8.84 ± 0.05	0.5	1	2
4	LDT243	8.39 ± 0.10	8.13 ± 0.06	8.11 ± 0.08	0.5	1	2
5	LDT244	8.89 ± 0.06	7.91 ± 0.15	8.23 ± 0.17	0.2	2	9.5
6	LDT245	9.10 ± 0.08	8.89 ± 0.01	8.79 ± 0.09	0.5	1	2
7	LDT451	8.27 ± 0.11 8.38 ± 0.11 ^d	8.03 ± 0.09	8.33 ± 0.11	1	2	2
8	LDT452	8.29 ± 0.14	7.94 ± 0.02	8.59 ± 0.16	2	5	2
9	LDT453	8.87 ± 0.07	8.92 ± 0.12	9.46 ± 0.06	4	0.3	1
11	LDT455	9.55 ± 0.13	8.74 ± 0.21	9.12 ± 0.05	0.4	2	6.5
Tamsulosin		9.46 ± 0.13 ^c	9.30 ± 0.08 ^c	10.00 ± 0.10 ^c	3.5	5	1.5

^a pK_B values (\pm SEM) calculated according to van Rossum.

^b Calculated by the antilog of the difference between pK_B values at different α_1 -adrenoceptor subtypes.

^c Data from ref 14.

^d pA_2 value \pm S.E., calculated from Schild plot constraining the slope to -1.

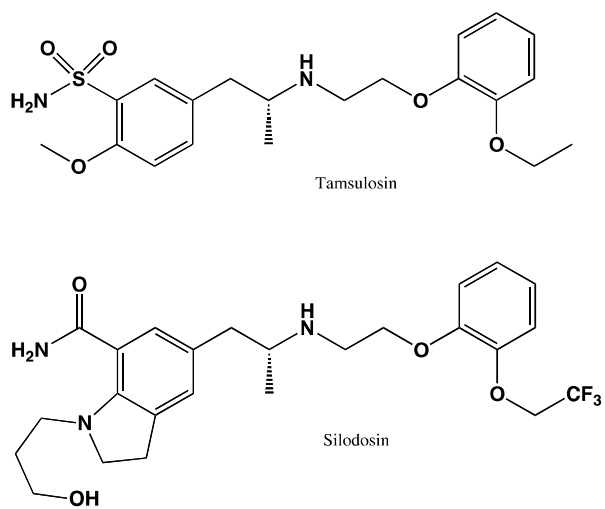
Figure 1. Chemical structures of α 1-adrenoceptor antagonists licensed for BPH.

Figure 2. Main interactions stabilizing the two putative (and specular) binding modes as computed between $\alpha 1a$ and **9**; A: Main interactions stabilizing the complex involving Asp106; B: Main interactions stabilizing the complex involving Glu180.

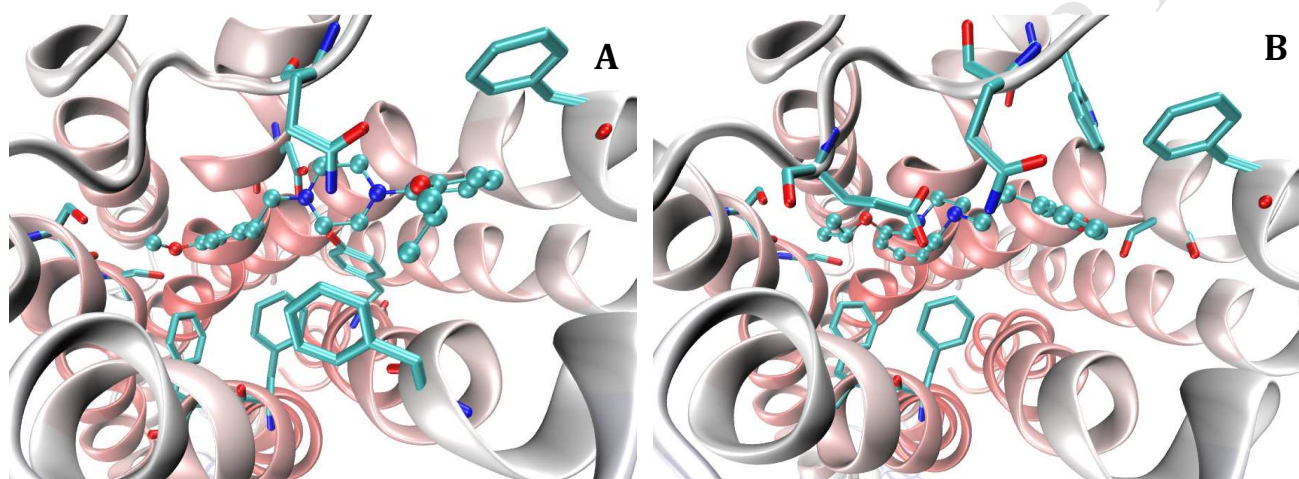
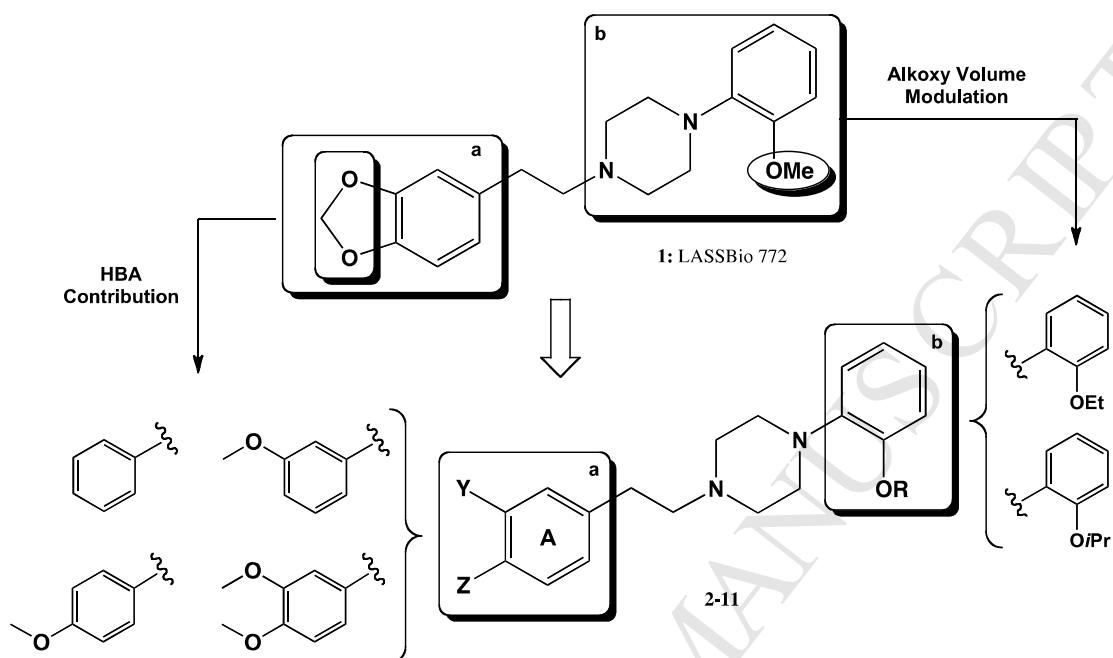
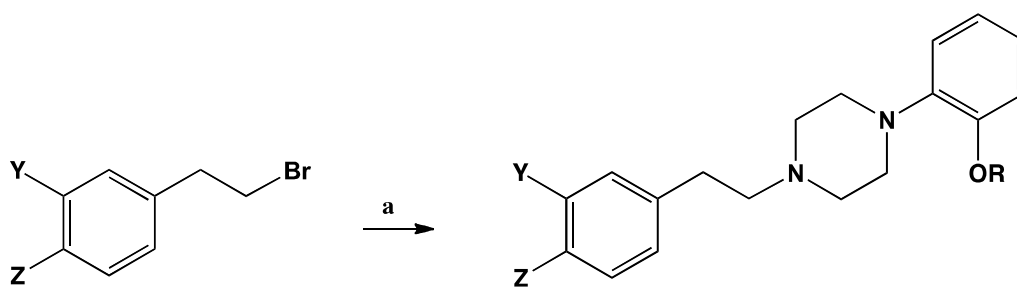


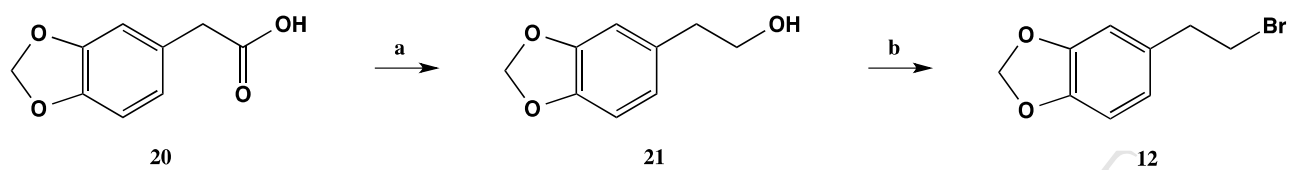
Chart 1. Design strategy to phenylpiperazines 2-11.

Scheme 1^a

12: Y = Z = -OCH₂O-
13: Y = Z = H
14: Y = OMe; Z = H
15: Y = H; Z = OMe
16: Y = Z = OMe

2: Y = Z = H; R = Me
3: Y = Z = -OCH₂O-; R = Et
4: Y = OMe; Z = H; R = Et
5: Y = H; Z = OMe; R = Et
6: Y = Z = OMe; R = Et
7: Y = Z = -OCH₂O-; R = *i*Pr
8: Y = Z = H; R = *i*Pr
9: Y = OMe; Z = H; R = *i*Pr
10: Y = H; Z = OMe; R = *i*Pr
11: Y = Z = OMe; R = *i*Pr

^aReagents and conditions: (a) 1-(2-alkoxyphenyl)piperazines, Et₃N, CH₃CN, MW irradiation 2.45 GHz, 450 W, 4 minutes, 93% (**2**), 93% (**3**), 68% (**4**), 84% (**5**), 69% (**6**), 80% (**7**), 82% (**8**), 40% (**9**), 52% (**10**), 55% (**11**).

Scheme 2^a

^aReagents and conditions: (a) LiAlH_4 , THF, r.t., 4h, 98%; (b) CBr_4 , triphenylphosphine, CH_3CN , r.t., 24 h, 76%.

Highlights

- 11 new phenylpiperazines derived from LASSBio 772 has been designed and synthesized
- Affinities for human α_1 -AR subtypes in radioligand binding assays were assessed
- Antagonist profiles at α_1 -AR subtypes in functional bioassays were evaluated
- Among the newly synthesized compounds, potent ligands were identified
- SAR-analysis identified new hits for further search for improved α_1 -AR agents